V European Conference on Computational Fluid Dynamics
ECCOMAS CFD 2010
J. C. F. Pereira and A. Sequeira (Eds)
Lisbon, Portugal,14-17 June 2010

A FIXED EULERIAN MESH-BASED SCHEME USING LEVEL SET FUNCTION FOR AIRBAG DEPLOYMENT SIMULATION INCLUDING THE EFFECT OF OUTSIDE AIR

Gaku Hashimoto*[*] and Kenji Ono[†]

[*]RIKEN (The Institute of Physical and Chemical Research)
2-1 Hirosawa, Wako-shi, Saitama 351-0198, JAPAN
e-mail: ghashimoto@riken.jp
[†]RIKEN (The Institute of Physical and Chemical Research)
2-1 Hirosawa, Wako-shi, Saitama 351-0198, JAPAN
e-mail: keno@riken.jp

Key words: Fluid-structure interaction, Eulerian mesh, Level set, Airbag deployment, Large deformation

Abstract. *We develop a coupling method to solve airbag deployment problems where a large-deformable thin structure moves in a high-speed flow field and inflation of the airbag influences variation of the interior and exterior fluid pressures. We have proposed a partitioned-solution coupling method based on a fixed Eulerian mesh with the level set function to predict the interior pressure distribution of an airbag. However it is necessary to include the effect of the exterior air because passenger's eardrum-splitting results from rapid variation of the exterior pressure. As a large-deformation fluid-structure interaction problem, we deal with a coupled problem of a gas flow and an unfolded airbag. It is confirmed that the moving airbag decreases the exterior fluid pressure and the vertical velocity of the airbag becomes larger accordingly.*

1 INTRODUCTION

Highly accurate analyses of mechanical interactions such as fluid-structure interactions (FSI) are important for elucidating complex physical phenomena in fields such as automotive engineering, civil engineering, aerodynamics, and biomechanics. Various FSI simulation methods have recently been developed and applied[1]. This study describes a fluid-structure coupling method for application to large-deformation FSI problems such as airbag deployment simulations where accurate simulation is necessary for human safety. After car impact, a high-speed inviscid compressible air flow, with high density and high pressure, enters an airbag rapidly and inflates it due to aerodynamic force.

We have proposed a partitioned-solution (iterative-staggered) coupling method based on a fixed Eulerian mesh with the level set function to predict the interior pressure distribution of an airbag[2]. Various Lagrangian-Eulerian coupling methods have recently been developed[3,4,5,6]. As the difference from these methods, our algorithm has characteristics of generation of the accurate level set function and application of Dirichlet boundary conditions for the fluid solver by using the level set function and the derivatives so as to satisfy the kinematic condition.

It is necessary to include the effect of the exterior air because passenger's eardrum-splitting results from rapid variation of the exterior pressure. In this study, we develop a coupling method to solve airbag deployment problems where a large-deformable thin structure moves in a high-speed flow field and inflation of the airbag influences variation of the interior and exterior fluid pressures.

2 GOVERNING EQUATIONS

The structure is assumed to be compressible and elastic. The equations of motion, using a Lagrangian description, are employed to obtain the displacement $\boldsymbol{u}$, velocity $\boldsymbol{v}$, and acceleration $\boldsymbol{a}$. The material is specified by giving the second Piola-Kirchhoff stress tensor according to the constitutive law for St. Venant-Kirchhoff materials.

The fluid is assumed to be a compressible, inviscid, and adiabatic ideal gas. The continuity equation, equations of motion, and pressure equation, using an Eulerian description, are employed to obtain the density ρ, velocity $\boldsymbol{v}$, and pressure p. In this study, it is necessary to obtain the derivatives of these fluid variables to enable use of the constrained interpolation profile finite element method (CIP-FEM)[7].

The boundary conditions at the fluid-structure interface are kinematic and dynamic coupling conditions. Because no mass flow across the interface is assumed, the normal velocities at the interface must match. The kinematic condition is

$$\boldsymbol{n} \cdot \boldsymbol{v}_{\mathrm{f}} = \boldsymbol{n} \cdot \frac{d\boldsymbol{u}_{\mathrm{s}}}{dt} \tag{1}$$

where $\boldsymbol{n}$ is the unit vector normal to the interface, $\boldsymbol{v}_{\mathrm{f}}$ is the fluid velocity, and $\boldsymbol{u}_{\mathrm{s}}$ is the structural displacement. It is necessary for the traction vectors to be equal so as to enforce equilibrium of forces at the fluid-structure interface. The dynamic conditions are

$$-p\,\boldsymbol{n} = \boldsymbol{n} \cdot \boldsymbol{T}_{\mathrm{s}} \tag{2}$$

where $\boldsymbol{T}_{\mathrm{s}}$ is the structural Cauchy stress tensor.

3 COMPUTATIONAL METHODS

Figure 1 shows a schematic diagram of the computational domains and meshes. The computational domains consist of the involved physical fluid domain Ω_{f}, structural domain Ω_{s}, and the void (that is, fictitious fluid) domain Ω_{v}. In the void domain, the Dirichlet boundary conditions for the fluid variables are applied to satisfy the kinematic condition. The computational meshes are divided into an overlapping, moving Lagrangian mesh for the structural domain and a fixed Eulerian mesh for the fluid and void domains. As a

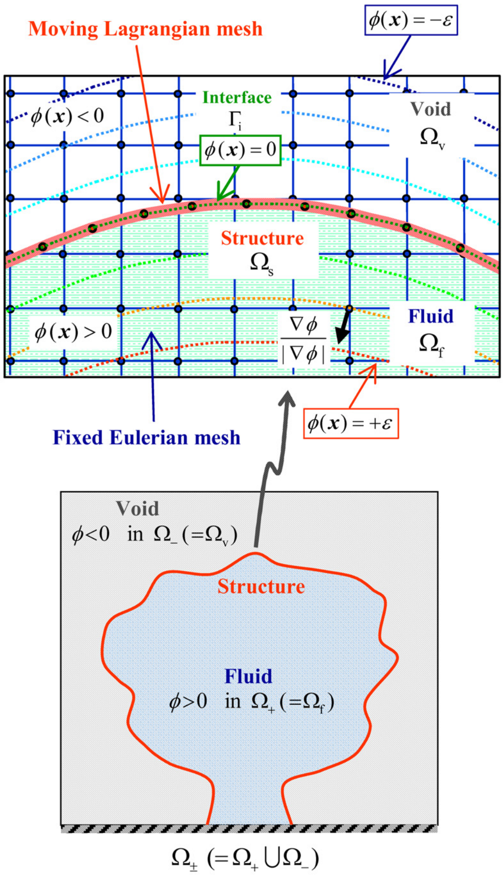

Figure 1: Computational domains and meshes

structural mesh, we use the 4-node mixed interpolation of tensorial components (MITC) shell elements by Dvorkin and Bathe[8]. As a fluid mesh, we use 8-node hexahedral elements for the CIP-FEM[7]. Because the structure is assumed to be sufficiently thin, the mid-surface of the structure corresponds to the fluid-structure interface Γ_{i}. The geometrical shapes of the deformable mid-surface are represented as a zero isosurface of the level set function $\phi(\boldsymbol{x})$ on the fluid mesh. In addition, the edges of the structure are always located on the outside boundary of the fixed Eulerian mesh. Then the fluid domain Ω_{f} and void domain Ω_{v} correspond to Ω_+ and Ω_- respectively.

$$\begin{cases} \phi(\boldsymbol{x}) > 0 & \forall \boldsymbol{x} \in \Omega_+ \\ \phi(\boldsymbol{x}) = 0 & \forall \boldsymbol{x} \in \Gamma_{\mathrm{i}} \\ \phi(\boldsymbol{x}) < 0 & \forall \boldsymbol{x} \in \Omega_- \end{cases} \tag{3}$$

The algorithm uses block Gauss-Seidel coupling iterations and combines advanced Eulerian fluid and Lagrangian structure solvers—specifically, the CIP method for the advection term of a fluid and the MITC shell elements for a large-deformable thin elastic structure.

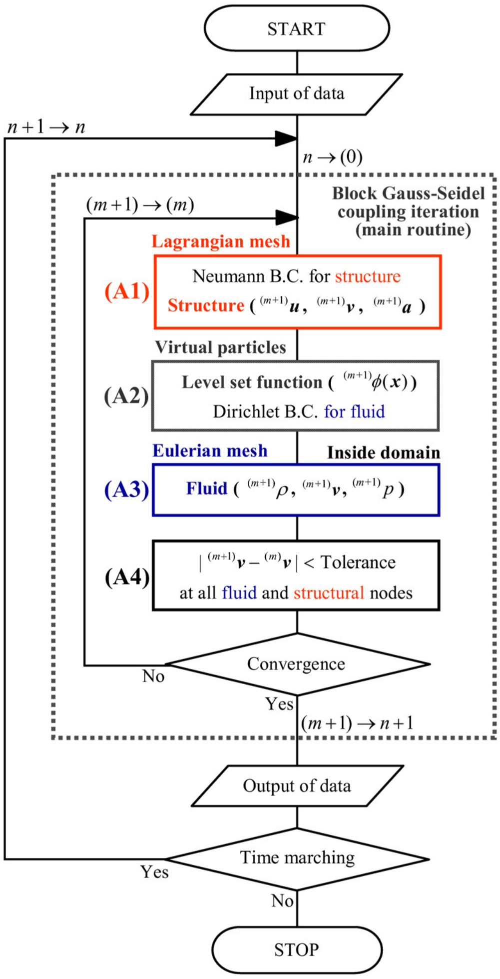

Figure 2: Partitioned-solution coupling method (n: time step; (m): iteration)

We express the large-deformable interface as a zero isosurface of the level set function and introduce an interface treatment technique to enforce the interfacial kinematic condition for interior fluid domains. Figure 2 shows the algorithm of our conventional method[2], which is summarized as follows:

(A1) Obtain the traction

$$\boldsymbol{n} \cdot \boldsymbol{T}_{\mathrm{s}} = -p\,\boldsymbol{n} \tag{4}$$

as the Neumann boundary conditions for the structural variables by interpolating from the fluid pressures $p(\boldsymbol{x}_{\mathrm{s}}^{I})$ at structural nodes $\boldsymbol{x}_{\mathrm{s}}^{I}$. The fluid pressures at the structural nodes are

$$p(\boldsymbol{x}_{\mathrm{s}}^{I}) \simeq \begin{cases} p_h(\boldsymbol{x}_{\mathrm{s}}^{I}) & \text{on the fluid side} \\ p_{\mathrm{v}} & \text{on the void side} \end{cases} \tag{5}$$

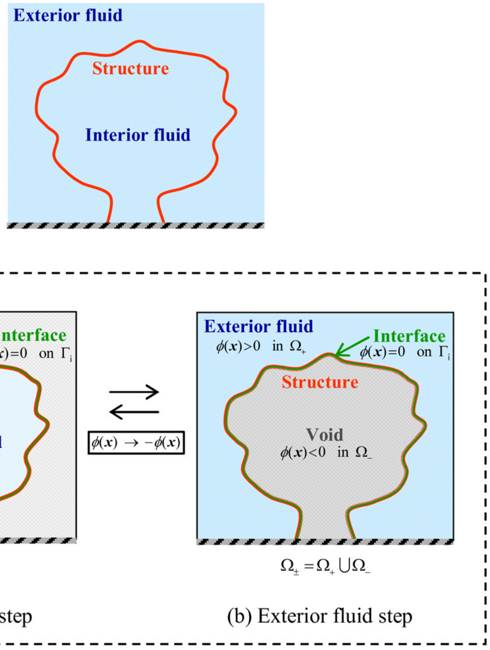

Figure 3: Computational domains

where $p_h(\boldsymbol{x}_\mathrm{s}^I)$ denotes the moving least squares (MLS) approximation from the sampling data of fluid pressure p^J, and p_v is the pressure in the void domain. Compute the structural displacement $\boldsymbol{u}$, velocity $\boldsymbol{v}$, and acceleration $\boldsymbol{a}$.

(A2) Generate the level set function $\phi(\boldsymbol{x})$ on the fluid mesh and apply the Dirichlet boundary conditions for the fluid variables in the void domain using the level set function and the derivatives.

(A3) Compute the fluid density ρ, velocity $\boldsymbol{v}$, and pressure p.

(A4) If the velocities at all fluid and structural nodes converge, proceed to the next time step.

In this study, we handle the fluid domains on both sides of the structure (Fig. 3, upper figure) so that we can predict pressure variation on the outside. Computation for the fluid domains is separated into interior and exterior fluid steps (Fig. 3, lower figures). To obtain the fluid variables on the inside of the structure, we follow the above-mentioned coupling method. To obtain the fluid variables on the outside of the structure, we reverse the sign of the level set function that has been already obtained ($-\phi(\boldsymbol{x}) \rightarrow \phi(\boldsymbol{x})$) and the Dirichlet boundary conditions for the exterior fluid variables are provided in the interior void domain. As shown in Fig. 4, two steps (B4) and (B5) are added to Fig. 2. The algorithm of the new coupling method is summarized as follows:

(B1) Obtain the traction as the Neumann boundary conditions for the structural variables by interpolating from the fluid pressures $p(\boldsymbol{x}_\mathrm{s}^I)$ at structural nodes $\boldsymbol{x}_\mathrm{s}^I$. The fluid

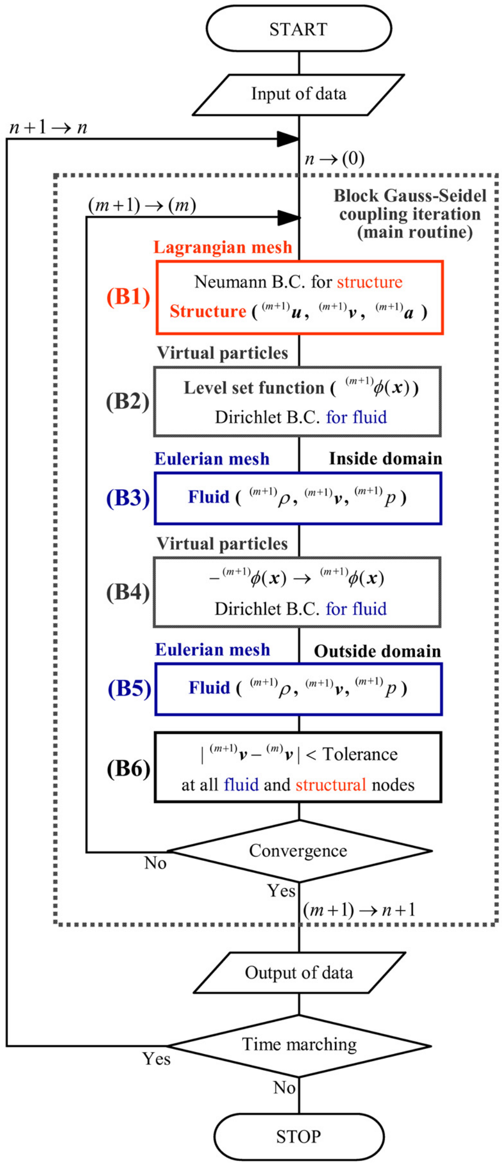

Figure 4: Partitioned-solution coupling method (n: time step; (m): iteration)

pressures at the structural nodes are

$$p(\boldsymbol{x}_{\mathrm{s}}^{I}) \simeq \begin{cases} (p_{\mathrm{in}})_h(\boldsymbol{x}_{\mathrm{s}}^{I}) & \text{on the fluid side} \\ (p_{\mathrm{ex}})_h(\boldsymbol{x}_{\mathrm{s}}^{I}) & \text{on the void side} \end{cases} \tag{6}$$

where $(p_{\mathrm{in}})_h(\boldsymbol{x}_{\mathrm{s}}^{I})$ and $(p_{\mathrm{ex}})_h(\boldsymbol{x}_{\mathrm{s}}^{I})$ denote the MLS approximations from the sampling data of interior and exterior fluid pressures p^J respectively. Compute the structural

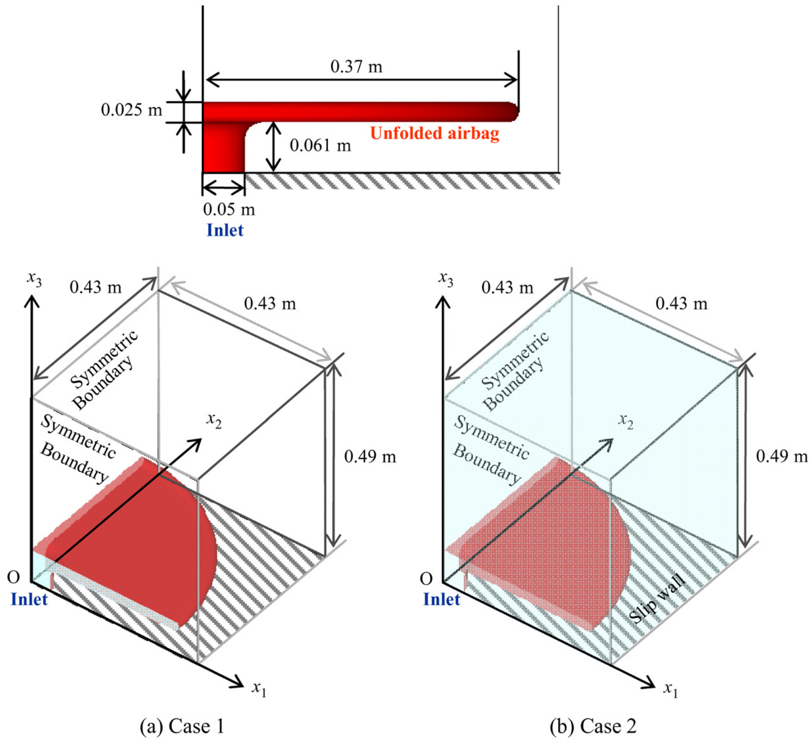

Figure 5: 3D analysis models of an air/thin-elastic-structure (airbag) system

displacement $\boldsymbol{u}$, velocity $\boldsymbol{v}$, and acceleration $\boldsymbol{a}$.

(B2) Generate the level set function $\phi(\boldsymbol{x})$ on the fluid mesh and apply the Dirichlet boundary conditions for the interior fluid variables in the exterior void domain using the level set function.

(B3) Compute the interior fluid density ρ, velocity $\boldsymbol{v}$, and pressure p.

(B4) Reverse the sign of the level set function $\phi(\boldsymbol{x})$ on the fluid mesh and apply the Dirichlet boundary conditions for the exterior fluid variables in the interior void domain using the level set function and the derivatives.

(B5) Compute the exterior fluid density ρ, velocity $\boldsymbol{v}$, and pressure p.

(B6) If the velocities at all fluid and structural nodes converge, proceed to the next time step.

3.1 NUMERICAL RESULTS AND DISCUSSION

Figure 5 shows 3D analysis models of stationary air and a flat airbag. Case 1 is an analysis model for the fluid domain on the inside of the airbag (Fig. 5, upper figure), and Case 2 is an analysis model for the fluid domains on both sides of the airbag (Fig. 5,

Symbol	Meaning	Value
${}^0\rho$	Initial density	1.3 $\mathrm{kg/m^3}$
${}^0p$	Initial pressure	1.0 atm
κ	Specific heat ratio	1.4
ρ_{inlet}	Inlet density	16.0 $\mathrm{kg/m^3}$
v_{inlet}	Inlet velocity	73.0 m/s
p_{inlet}	Inlet pressure	12.0 atm

Table 1: Parameters of air

Symbol	Meaning	Value
${}^0\rho$	Initial density	1.0×10^3 $\mathrm{kg/m^3}$
a	Thickness	7.3×10^{-4} m
E	Young's modulus	6.0×10^9 Pa
ν	Poisson's ratio	0.3

Table 2: Parameters of elastic structure

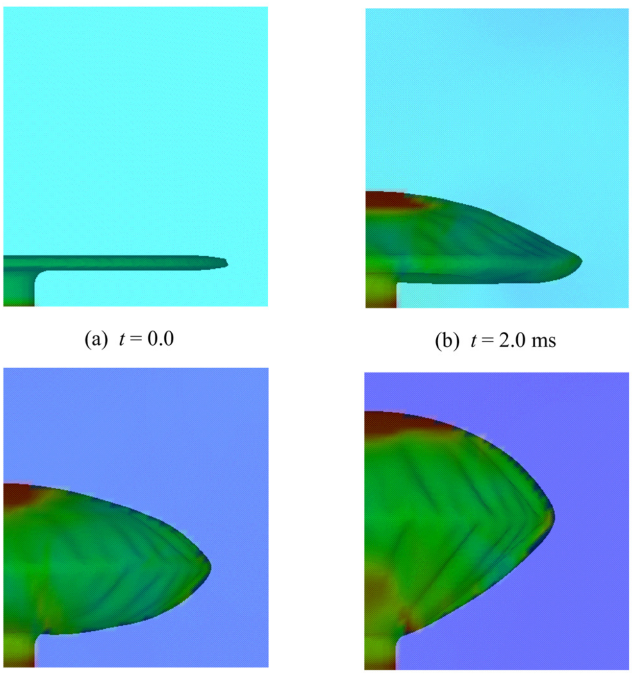

(a) $t = 0.0$ (b) $t = 2.0$ ms (c) $t = 4.0$ ms (d) $t = 6.0$ ms

Figure 6: Pressure contours and zero level set on the fluid mesh in Case 2 (the present method including the effect of outside air)

lower figure). An air flow with high density and high pressure enters the flat airbag from a bottom inlet. We set the geometry of this model and the parameters by referring to the model data of 3D unfolded airbag deployment simulation by Cirak and Radovitzky[3]. A symmetric boundary condition is applied on the left and front boundaries and a slip condition is applied on the bottom boundary except at the inlet. Tables 1 and 2 show the parameters for the compressible inviscid air and a thin elastic structure. The void pressure is 1.0 atm for Case 1. Figure 6 shows the pressure contours with a zero isoline of the level set function on the fluid mesh for Case 2. The airbag inflates because aerodynamic force acts on the top wall, and the side wall moves toward the center of the airbag. In Case 2, an outflow of the exterior air decreases the exterior fluid pressure. As a result, the vertical velocity at the center point of the airbag for Case 2 becomes larger than for Case 1.

4 CONCLUSIONS

We developed a partitioned-solution (iterative-staggered) coupling method to solve airbag deployment problems where a large-deformable thin structure moves in a high-speed flow field and inflation of the airbag influences variation of the interior and exterior fluid pressures. In the coupled problem of a gas flow and an unfolded airbag, we confirmed that the moving airbag decreases the exterior fluid pressure and the vertical velocity of the airbag becomes larger accordingly.

ACKNOWLEDGEMENTS

This research was supported by a Grant-in-Aid for Young Scientists (B) (21760064) in 2009-2010, Ministry of Education, Culture, Sports, Science and Technology. The calculations were performed by using the RIKEN Integrated Cluster of Clusters (RICC) facility. We gratefully acknowledge these supports.

REFERENCES

[1] H.J. Bungartz and M. Schafer, Fluid-Structure Interaction, Modeling, Simulation, Optimization, Springer, (2007).

[2] G. Hashimoto, K. Ono and H. Noguchi, Proceedings of WCCM8 & ECCOMAS2008 (CD-ROM), Italy, Venice, (2008).

[3] F. Cirak and R. Radovitzky, *Computers & Structures*, **83**, 491–498, (2005).

[4] A. Legay, J. Chessa and T. Belytschko, *Comput. Methods Appl. Mech. Engrg.*, **195**, 2070–2087, (2006).

[5] T. Sawada, S. Nakasumi and A. Tezuka, Proceedings of WCCM8 & ECCOMAS2008 (CD-ROM), Italy, Venice, (2008).

[6] A. Gerstenberger and W.A. Wall, *Comput. Methods Appl. Mech. Engrg.*, **197**, 1699–1714, (2008).

[7] T. Jimbo and T. Tanahashi, Proceedings of ICCM2004, Singapore, (2004).

[8] E. Dvorkin and K. J. Bathe, *Eng. Comput.*, **1**, 77–88, (1984).